Quantum statistical mechanics of vortices in high-temperature superconductors

G. Blatter
Theoretische Physik, Eidgenössische Technische Hochschule Zürich–Hönggerberg, CH-8093 Zürich, Switzerland

B. I. Ivlev*
Theoretische Physik, Eidgenössische Technische Hochschule Zürich–Hönggerberg, CH-8093 Zürich, Switzerland
and L. D. Landau Institute for Theoretical Physics, 117940 Moscow, Russian Federation
(Received 7 September 1993; revised manuscript received 6 June 1994)

Starting from the vortex equation of motion, we construct an effective Euclidean action and formulate the quantum statistical mechanics of the vortex system. The formalism is applied to the calculation of various thermodynamic quantities such as the specific heat and the magnetic susceptibility of the vortex lattice. Furthermore, we investigate the effect of quantum fluctuations on the vortex-lattice melting transition.

I. INTRODUCTION

A realistic description of the phenomenology of high-temperature superconductors requires one to go beyond the mean-field level and to take fluctuations into account.[1,2] The special material parameters of the oxide superconductors, their large transition temperature T_c implying a short (in-plane) coherence length ξ, as well as the large effective-mass anisotropy ratio $M/m = 1/\varepsilon^2 \gg 1$, strongly enhance the importance of thermal fluctuations, leading to phenomena such as the melting of the vortex lattice[3–7] or the appearance of giant creep.[8] Quantitatively, the importance of thermal fluctuations is determined by the Ginzburg number $G \propto T_c^4/\varepsilon^2$, which is about six orders of magnitude larger in the oxides than in conventional superconductors.[2] From a more general point of view, fluctuations need not be based on a thermal source but can be of quantum origin as well. The observation[9–11] of a strong magnetic relaxation at very low temperatures has demonstrated the importance of quantum effects in the phenomenology of high-temperature superconductors. The theoretical analysis of these experiments in terms of the quantum creep theory[12,13] shows that the relevant parameter determining the importance of quantum effects is the dimensionless sheet resistance $Q=(e^2/\hbar)(\rho_N/d)$, where ρ_N is the (in-plane) normal-state resistivity and d is the layer separation (for the case of Hall tunneling[14] the parameter is $Q=1/dn_s\xi^2$ with n_s the superfluid density). Again, this parameter is by orders of magnitude larger in the high-T_c superconductors as compared with the corresponding quantity in conventional superconductors. The question can then be posed whether the quantum creep phenomena are the only manifestation of quantum effects in the copper oxide superconductors. In this paper we show that quantum fluctuations can play an important role in the statistical mechanics of the vortex system, suggesting that the usual classical statistical mechanics description should be replaced by the more general quantum formulation in many cases.

Below we analyze the consequences of quantum effects for the statistical mechanics properties of the vortex system. We calculate the contribution of (quantum) fluctuations to thermodynamic quantities such as the specific heat of the vortex system and the reversible magnetization, and we determine their effect on the melting transition, particularly on the shape of the melting line. A short account of the latter topic has been presented in Ref. 15. Results on the specific heat and on the reversible magnetization have been obtained recently by Bulaevskii and co-workers.[16,17] Here we extend their result for the specific heat obtained for a layered superconductor in the high-field limit in various directions: we determine the corresponding expression for a dissipative dynamics in the low-field case (the same result applies to the continuous anisotropic situation) and we consider the case of a pure Hall-type dynamics where the vortex system develops undamped modes (Tkachenko modes). In the dissipative situation the low-temperature specific heat picks up a linear-in-T contribution from the vortex system, whereas for the Hall dynamics we obtain a $T^{1/2}$ contribution for the single-vortex fluctuation regime. These terms have to compete with the specific-heat contributions from various other sources such as impurities or the quasiparticle contribution from states within the vortex cores, rendering the experimental identification of the vortex part in the specific heat difficult. Second, we present a derivation for the reversible magnetization which takes dispersive effects in the vortex dynamics into account. Within a mean-field (London) theory the reversible diamagnetic response is predicted to follow the logarithmic behavior $-4\pi M \propto \ln H$ in the intermediate-field regime. Quantum fluctuations lead to a reduction in the diamagnetic response and we find good agreement between the theoretical analysis and the experimental results.[17] Regarding the melting transition we find that quantum fluctuations do play a role at low temperatures and high magnetic fields and we obtain good agreement between experimentally measured melting lines and line shapes calculated on the basis of the Lindemann criterion.

We are then in a situation where we wish to explain a

variety of different experiments (quantum creep, reversible diamagnetic response, vortex-lattice melting transition) within one theoretical framework invoking quantum fluctuations in the explanation of these phenomena. As quantum effects are quantified by the parameter Q we can check for the consistency of our approach by using only one set of parameters in the description of the different experimental results and we will show below that this goal indeed can be reached.

The inclusion of quantum fluctuations requires one to go beyond the static description and to adopt a dynamic formalism. In Sec. II we give a brief introduction to the quantum statistical mechanics of the vortex system in a type-II superconductor. We extend the classical formalism based on the continuum elastic theory for the vortex lattice and involving the configurational energy to a dynamic formalism based on the (Euclidean) action. The dynamic component in the action is obtained via the vortex equation of motion and we briefly discuss the structure of the latter, including the possibility of a Hall component in the vortex motion as well as the occurrence of dispersive effects in the transport coefficients. In Sec. III we apply this formalism to the calculation of the specific heat C_v of the vortex system and we determine the magnetic "susceptibility" $dM/d\ln B$. Our analysis of quantum statistical effects differs from that of Bulaevskii and co-workers[16,17] as we account for dispersive effects in the transport coefficients. The latter are expected to be relevant in clean-limit superconductors such as the copper oxide materials. In Sec. IV we concentrate on the melting transition of the vortex lattice and calculate the corrections to the melting line arising from the quantum component in the vortex motion within the Lindemann approximation. We critically examine various (approximate) expressions for the melting line in comparison with experimental data[18] on the melting line covering a large range in magnetic field and involving different materials such as $YBa_2Cu_3O_{7-y}$ (YBCO),[7,18-20] and $Bi_2Sr_2CaCu_2O_8$ (BiSCCO).[21] We find that satisfactory agreement over a large field range can be obtained if the suppression of the order parameter[5] on approaching the upper critical field line H_{c_2} as well as quantum effects are included in the determination of the melting line.

II. FORMALISM

We consider either a uniaxially anisotropic or a layered type-II superconductor characterized by the planar penetration depth λ and the planar coherence length ξ, $\kappa=\lambda/\xi\gg1$. The anisotropy is described by the effective-mass ratio $\varepsilon^2=m/M$, with m denoting the planar mass and M the effective mass along the (z) axis of the material, and d is the layer spacing. The starting point for the classical description of the vortex statistical mechanics is the free-energy functional within the continuum elastic approximation.[22] Denoting by $\mathbf{u}(\mathbf{r})$ the displacement field of the vortex system and adopting the usual Fourier representation

$$\mathbf{u}(\mathbf{k})=\int d^3r\, e^{-i\mathbf{k}\cdot\mathbf{r}}\mathbf{u}(\mathbf{r}) , \tag{1}$$

the free-energy functional $\mathcal{F}[\mathbf{u}]$ takes the form [$\mathbf{k}=(\mathbf{K},k_z)$, $\mathbf{K}_\perp=(k_y,-k_x)$]

$$\mathcal{F}[\mathbf{u}]=\frac{1}{2}\int\frac{dk_z}{2\pi}\int\frac{d^2K}{(2\pi)^2}\{c_{11}(\mathbf{k})[\mathbf{K}\cdot\mathbf{u}]^2+c_{66}[\mathbf{K}_\perp\cdot\mathbf{u}]^2 +c_{44}(\mathbf{k})[k_z\mathbf{u}]^2\} , \tag{2}$$

with $c_{11}(\mathbf{k})$, c_{66}, and $c_{44}(\mathbf{k})$ denoting the (dispersive) compression, shear, and tilt moduli. The $\mathbf{K}$ integration in (2) runs over the two-dimensional Brillouin zone, $K\le K_{BZ}\approx\sqrt{4\pi}/a_0$, $a_0\approx\sqrt{\Phi_0/B}$ is the vortex lattice constant, and the integration over the k_z component is limited by the condition $|k_z|<k_\infty\simeq1/\max(d,\varepsilon\xi)$. For the configuration $\mathbf{B}\|c$ the elastic moduli are given by (see Ref. 2 and references therein)

$$c_{44}(\mathbf{k})=c_{44}^0(\mathbf{k})+c_{44}^c(\mathbf{k}) , \tag{3}$$

$$c_{44}^0(\mathbf{k})=\frac{B^2}{4\pi}\frac{1}{1+\lambda^2(K^2/\varepsilon^2+k_z^2)} , \tag{4}$$

$$c_{44}^c(\mathbf{k})\approx\frac{\varepsilon_0}{2a_0^2}\left[\varepsilon^2\ln\frac{\kappa^2/\varepsilon^2}{1+\lambda^2K_{BZ}^2/\varepsilon^2+\lambda^2k_z^2} +\frac{1}{\lambda^2k_z^2}\ln\left[1+\frac{\lambda^2k_z^2}{1+\lambda^2K_{BZ}^2}\right]\right] , \tag{5}$$

$$c_{11}(\mathbf{k})=\frac{1+\lambda^2k^2/\varepsilon^2}{1+\lambda^2k^2}c_{44}^0(\mathbf{k}) , \tag{6}$$

$$c_{66}=\frac{\Phi_0B}{(8\pi\lambda)^2} , \tag{7}$$

where the line energy scale ε_0 is given by

$$\varepsilon_0=\left[\frac{\Phi_0}{4\pi\lambda}\right]^2 , \tag{8}$$

with $\Phi_0=hc/2e$ the unit of flux. Close to the Brillouin-zone boundary the tilt modulus is dominated by the single-vortex-line tension $\varepsilon_l(k_z)=a_0^2c_{44}^c(k_z)$ and for a strongly layered material the (ε-independent) electromagnetic term in c_{44}^c gives the dominant contribution. The classical statistical mechanics of the vortex system is given by the partition function

$$Z=\int\mathcal{D}[\mathbf{u}]\exp[-\mathcal{F}[\mathbf{u}]/T] . \tag{9}$$

In order to go over to a quantum statistical description of the vortex system we have to replace the free-energy functional by the Euclidean action $\mathcal{S}[\mathbf{u}]$, which now also involves a dynamical contribution. This dynamical term is related to the vortex equation of motion via the usual Euler-Lagrange variational principle and thus we can find the desired action functional once we know the expression for the vortex equation of motion.

A microscopic derivation of the vortex equation of motion in the presence of scattering has been given by Kopnin and Kravtsov[23,24] and by Kopnin and Salomaa.[25] In the resulting equation the driving Lorentz force $(\Phi_0/c)\mathbf{j}\times\mathbf{n}$ is balanced against the friction force $\eta_l\mathbf{v}_v$ and the Hall force $\alpha_l\mathbf{v}_v\times\mathbf{n}$,

$$\frac{\Phi_0}{c}\mathbf{j}\times\mathbf{n}=\eta_l\mathbf{v}_v+\alpha_l\mathbf{v}_v\times\mathbf{n}\ . \tag{10}$$

In (10) the vortex velocity $\mathbf{v}_v$ is defined with respect to laboratory frame of reference. In the low-frequency limit the transport coefficients η_l and α_l take the form[25]

$$\eta_l=\frac{\Phi_0}{c}\rho_s\frac{3}{2}\int_0^{\pi/2}d\theta\sin^3\theta\frac{\omega_0(\theta)\tau_r}{1+[\omega_0(\theta)\tau_r]^2}\ ,$$
$$\alpha_l=\frac{\Phi_0}{c}\rho_s\frac{3}{2}\int_0^{\pi/2}d\theta\sin^3\theta\frac{[\omega_0(\theta)\tau_r]^2}{1+[\omega_0(\theta)\tau_r]^2}\ . \tag{11}$$

Here, $\omega_0(\theta)\simeq v_F\partial_R\Delta(R)/2\varepsilon_F\sin\theta$ is the level separation between the quantized states in the vortex core (see, e.g., Caroli, De Gennes, and Matricon[26]), which depends on the angle θ enclosed by the quasiparticle momentum and the vortex axis. The order parameter $\Delta(R)$ carries the dimension of energy ($\Delta_\infty=\hbar v_F/\pi\xi_0$). Furthermore, $\rho_s=2e|\Psi_0|^2$ is the superfluid density, τ_r is the scattering relaxation time, v_F is the Fermi velocity, and ε_F the Fermi energy. The main contribution to the integral in (11) arises from large angles. In the following we will ignore the angular dependence of ω_0 and use the estimate $\hbar\omega_0\simeq T_c^2/\varepsilon_F$. Note that no term of the form $\eta_l'\mathbf{v}_s$ appears in (10)—such a term would lead to a deceleration of the superflow even for vortices at rest.[27]

We present a simple (heuristic) argument for the form of the vortex equation of motion (10) in the presence of scattering. The argument is based on the requirement that the resulting vortex velocity $\mathbf{v}_v$ has to be consistent with the carrier motion inside the vortex core.[28,25] The latter is described by the generalized law of conductivity in the presence of both an electric ($\mathbf{E}$) and a magnetic field ($\mathbf{B}$); for $\mathbf{B}\|\mathbf{n}$ and $\mathbf{j},\mathbf{E}\perp\mathbf{n}$ we can write

$$\mathbf{j}=\sigma_\parallel\mathbf{E}+\sigma_\perp\mathbf{n}\times\mathbf{E}\ , \tag{12}$$

with

$$\sigma_\parallel=\sigma_N\frac{1}{1+\nu^2}\quad\text{and}\quad\sigma_\perp=\sigma_N\frac{\nu}{1+\nu^2}\ , \tag{13}$$

and the conductivity is given by $\sigma_N=e^2n\tau_r/m$ (n is the free-carrier density). The relaxation time τ_r accounts for all the scattering processes and the parameter $\nu=\omega_c\tau_r$ relates to the Hall effect with $\omega_c=eB/mc$ the cyclotron frequency. Rewriting the electric field $\mathbf{E}$ in terms of the vortex velocity $\mathbf{v}_v$, $\mathbf{E}=\mathbf{B}\times\mathbf{v}_v/c$, and taking the cross product of (12) with $\Phi_0\mathbf{n}/c$, we obtain the force equation

$$\frac{\Phi_0}{c}\mathbf{j}\times\mathbf{n}=\tilde{\eta}_l\mathbf{v}_v+\tilde{\alpha}_l\mathbf{v}_v\times\mathbf{n}\ , \tag{14}$$

with the two transport coefficients $\tilde{\eta}_l=\pi\hbar n\nu/(1+\nu^2)$ and $\tilde{\alpha}_l=-\pi\hbar n\nu^2/(1+\nu^2)$ describing the dissipative and the Hall component of the motion (we have used $\sigma_N\Phi_0B/c^2=\pi\hbar n\nu$). For an electron in a magnetic field B the parameter ν is determined by the cyclotron motion and hence involves the cyclotron frequency $\omega_c=eB/mc$. On the other hand, the corresponding frequency for an electron orbiting within the core of a vortex is given by the level spacing $\hbar\omega_0$. Substituting $\omega_c\to\omega_0$ and $-en\to\rho_s=2e|\Psi_0|^2$ in the expressions for the coefficients $\tilde{\eta}_l$ and $\tilde{\alpha}_l$, we recover the result (10) with the transport coefficients (11) derived from microscopic calculations.

Let us briefly discuss the various types of motion a vortex can perform on the basis of (10). In most cases the parameter $\omega_0\tau_r\ll1$ is small and the equation of motion is dominated by the dissipative term with the viscous drag coefficient η_l given by the Bardeen-Stephen expression[29]

$$\eta_l\approx\frac{\Phi_0^2\sigma_N}{2\pi c^2\xi^2}\ , \tag{15}$$

with σ_N the normal-state conductivity of the material. Equation (15) describes well the situation at low fields and low temperatures, whereas corrections become important near the transition temperature and for high magnetic fields.[30,31] In the limit $\alpha_l\ll\eta_l$, Eq. (10) then simplifies to

$$\eta_l\mathbf{v}_v=\frac{\Phi_0}{c}\mathbf{j}\times\mathbf{n}\ , \tag{16}$$

and the vortex moves at right angles with respect to the external current density j. On the other hand, in very pure material such that $\omega_0\tau_r\gg1$ [note that this corresponds to the superclean limit $l\gg\xi(\varepsilon_F/\Delta)$, where $l=v_F\tau_r$ denotes the mean free path and Δ is the gap parameter; this condition guarantees the existence of well-defined quasiparticle states in the core] the Hall term becomes the dominant one with

$$\alpha_l=\frac{\Phi_0}{c}\rho_s=\pi\hbar n\ , \tag{17}$$

where the last equation applies in the limit $T\to0$. In this case we recover the Magnus force as the only force acting on the vortex,

$$\frac{\Phi_0}{c}\rho_s(\mathbf{v}_s-\mathbf{v}_v)\times\mathbf{n}=\mathbf{0}\ , \tag{18}$$

which thus is dragged along with the superflow, the typical situation for a vortex in an uncharged superfluid ($\mathbf{v}_s$ is the velocity of the superfluid with respect to the laboratory frame of reference).

The more conventional situation in a superconductor involves a large dissipative and only a small Hall component in the vortex motion. However, in the oxide superconductors the smallness of ξ and ε_F and the largeness of $l=v_F\tau_r$ and Δ place these materials close to or even within the superclean limit with a non-negligible or even dominant Hall component in the equation of motion.

The results (11) apply to the quasistatic limit of the vortex motion. At finite frequencies dispersive effects lead to a reduction of the transport coefficients,[25]

$$\eta_l(\omega)\approx\frac{\Phi_0}{c}\rho_s\frac{\omega_0\tau_r(1-i\omega\tau_r)}{(1-i\omega\tau_r)^2+(\omega_0\tau_r)^2}\ ,$$
$$\alpha_l(\omega)\approx\frac{\Phi_0}{c}\rho_s\frac{(\omega_0\tau_r)^2}{(1-i\omega\tau_r)^2+(\omega_0\tau_r)^2}\ . \tag{19}$$

The above results are valid for frequencies $\omega < 2\Delta/\hbar$ and hence the dispersive effects are relevant in relatively clean material with $T_c\tau_r/\hbar \gtrsim 1$, such as, for example, the high-temperature superconductors. Away from the superclean limit (i.e., for $\omega_0\tau_r \ll 1$) or for high frequencies ($\omega\tau_r \gg 1$) the dissipative term dominates and we recover the Bardeen-Stephen result (15) with a dispersive conductivity $\sigma_N(\omega)$ of the Drude type.[32]

With the results (10) and (19) for the equation of motion we can easily construct an expression for the Euclidean action $\mathcal{S}[\mathbf{u}]$. The displacement field $\mathbf{u}(\tau)$ is $\hbar/T$-periodic on the imaginary time axis and we can go over to the Matsubara representation with

$$\mathbf{u}_n = \mathbf{u}(\omega_n) = \frac{T}{\hbar}\int_{-\hbar/2T}^{\hbar/2T} d\tau\, e^{i\omega_n\tau}\mathbf{u}(\tau) \tag{20}$$

and the Matsubara frequencies $\omega_n = 2\pi nT/\hbar$. The Euclidean action[33] $\mathcal{S}[\mathbf{u}]$ then takes the form

$$\frac{\mathcal{S}[\mathbf{u}]}{\hbar} = \frac{1}{T}\sum_n \{\mathcal{T}[\mathbf{u}_n] + \mathcal{F}[\mathbf{u}_n]\}\ , \tag{21}$$

with the dynamical term $\mathcal{T}[\mathbf{u}_n]$ given by

$$\mathcal{T}[\mathbf{u}_n] = \frac{1}{2}\int \frac{d^3k}{(2\pi)^3}[\mu\omega_n^2\mathbf{u}_n(\mathbf{k}) + \eta(\omega_n)|\omega_n|\mathbf{u}_n(\mathbf{k}) + \alpha(\omega_n)\omega_n\hat{\mathbf{z}}\times\mathbf{u}_n(\mathbf{k})]\mathbf{u}_{-n}(-\mathbf{k})\ , \tag{22}$$

and the elastic term $\mathcal{F}[\mathbf{u}_n]$ given by (2) above. The Matsubara expressions for the transport coefficients are obtained from the real-frequency expressions (19) via the substitution $\partial_t \leftrightarrow -i\omega \leftrightarrow |\omega_n|$ for a dissipative dynamics, whereas for a Hamiltonian dynamics the rule is $\partial_t \leftrightarrow -i\omega \leftrightarrow \omega_n$. The transport coefficients $\eta(\omega_n)$ and $\alpha(\omega_n)$ are simply the lattice equivalents of the single-vortex expressions (19), $\eta = \eta_l/a_0^2$ and $\alpha = \alpha_l/a_0^2$. Furthermore, we have introduced a (nondispersive) mass term (μ) for our later convenience here. The Euclidean action (21) allows us to formulate the quantum statistical mechanics of the vortex system on the basis of the partition function

$$\mathcal{Z} = \int \mathcal{D}[\mathbf{u}]\exp[-\mathcal{S}[\mathbf{u}]/\hbar]\ , \tag{23}$$

replacing its classical analogue (9).

The determination of the partition function (23) is complicated by the friction term which describes the coupling of the system to a reservoir. We can write the partition function $\mathcal{Z}$ as the product

$$\mathcal{Z} = \left[\frac{\int\mathcal{D}[\mathbf{u}]\exp[-\mathcal{S}/\hbar]}{\int\mathcal{D}[\mathbf{u}]\exp[-\mathcal{S}_0/\hbar]}\right]\int\mathcal{D}[\mathbf{u}]\exp[-\mathcal{S}_0/\hbar]\ , \tag{24}$$

with

$$\mathcal{S}_0[\mathbf{u}] = \frac{1}{2T}\int\frac{d^3k}{(2\pi)^3}\sum_n\{\mu|\omega_n|^2\mathbf{u}_n(\mathbf{k})\mathbf{u}_{-n}(-\mathbf{k}) + f[\mathbf{u}_n(\mathbf{k})]\} \tag{25}$$

the action for a set of conventional harmonic oscillators. Here, $f[\mathbf{u}_n(\mathbf{k})]$ is the free-energy contribution of the $\mathbf{k}$ mode as given by Eq. (2). The first factor in (24) does not depend on the measure and the second factor is easily calculated to be[34]

$$\mathcal{Z}_0 = \int\mathcal{D}[\mathbf{u}]\exp[-\mathcal{S}_0[\mathbf{u}]/\hbar] = \prod_{\mathbf{k}}\frac{T^2\mu}{\hbar^2\sqrt{\varepsilon_L\varepsilon_T}}\prod_{n=1}^{\infty}\left[1+\frac{\varepsilon_L}{\mu\omega_n^2}\right]^{-1}\left[1+\frac{\varepsilon_T}{\mu\omega_n^2}\right]^{-1}\ . \tag{26}$$

The elastic energies of the longitudinal and transverse elastic modes are

$$\varepsilon_L(\mathbf{k}) = c_{11}(\mathbf{k})K^2 + c_{44}(\mathbf{k})k_z^2\ ,\qquad \varepsilon_T(\mathbf{k}) = c_{66}K^2 + c_{44}(\mathbf{k})k_z^2\ . \tag{27}$$

The partition function $\mathcal{Z}$ of the vortex system then takes the form

$$\mathcal{Z} = \prod_{\mathbf{k}}\frac{T^2\mu}{\hbar^2\sqrt{\varepsilon_L\varepsilon_T}}\prod_{n=1}^{\infty}\left[\left[1+\frac{\eta(\omega_n)}{\mu|\omega_n|}+\frac{\varepsilon_L}{\mu\omega_n^2}\right]\times\left[1+\frac{\eta(\omega_n)}{\mu|\omega_n|}+\frac{\varepsilon_T}{\mu\omega_n^2}\right]+\frac{\alpha^2(\omega_n)}{\mu^2\omega_n^2}\right]^{-1}\ . \tag{28}$$

Using the result (28) we can find the free-energy density $f = -[T\ln\mathcal{Z}]/V$. Going over to the real-frequency axis via analytic continuation we obtain the following final expression for the free-energy density:

$$f = -T\int\frac{dk_z}{2\pi}\int_{\mathrm{BZ}}\frac{d^2K}{(2\pi)^2}\int_0^{\infty}\frac{d\omega}{\pi}\ln\left[2\sinh\frac{\hbar\omega}{2T}\right]\frac{\partial}{\partial\omega}\mathrm{Im}\ln\{[\mu\omega^2+\varepsilon_L-i\omega\eta(\omega)][\mu\omega^2+\varepsilon_T-i\omega\eta(\omega)]-\omega^2\alpha^2(\omega)\}\ . \tag{29}$$

In order to obtain the corresponding result for a single vortex line we have to drop the $\mathbf{K}$ integration in (29) and to make the substitutions $\varepsilon_{(L)T}\to\varepsilon_l k_z^2$, $\mu\to\mu_l$, $\eta\to\eta_l$, and $\alpha\to\alpha_l$. The (dispersive) line tension $\varepsilon_l(k_z)$ has been given above; see Eq. (5). The above results are valid for the case of dispersive transport coefficients $\eta(\omega)$ and $\alpha(\omega)$ as long as the generalized susceptibility (Green's function) has no singularities in the upper half plane for the

complex ω variable. For example, the power-law dispersion

$$\eta(\omega_n)=\eta(0)[1+(|\omega_n|/\Omega)^m]$$

with integer $m>1$ violates the causality principle since it does not satisfy this requirement.

Before turning to the quantum statistical mechanics of the vortex system we introduce here the two dimensionless parameters quantifying the importance of the thermal and of the quantum fluctuations: These parameters are the Ginzburg number G,

$$G=\frac{1}{2}\left[\frac{T_c}{H_c^2(0)\varepsilon\xi^3(0)}\right]^2=\frac{1}{8}\left[\frac{T_c}{\varepsilon\varepsilon_0(0)\xi(0)}\right]^2, \tag{30}$$

and the quantum sheet resistance Q

$$Q=\frac{e^2}{\hbar}\frac{\rho_N}{d}. \tag{31}$$

Here, the thermodynamic field $H_c(0)$, the coherence length $\xi(0)$, and the energy scale $\varepsilon_0(0)$ are all Ginzburg-Landau (GL) values extrapolated linearly to zero. Typical values for the Ginzburg number G and for the quantum sheet resistance Q in the high-temperature superconductors are $G\approx 4\times 10^{-3}$ and $Q\approx 0.2$ for the anisotropic YBCO material [we choose $\xi(0)\approx 13.5$ Å, $\lambda(0)\approx 1000$ Å, $\varepsilon\approx\frac{1}{5}$, $d\approx 12$ Å, and we estimate $\rho_N\simeq 10^{-4}$ Ω cm close to T_c; with decreasing temperature $Q\propto\rho_N(T)\propto T$ is reduced; at low temperatures $Q\approx 0.01$ consistently explains the magnitude of quantum creep[12]] and $G\approx 4$ for the layered BiSCCO superconductor [$\xi(0)\approx 20$ Å, $\lambda(0)\approx 1600$ Å, $\varepsilon\approx\frac{1}{100}$, $d=15$ Å]. The value for Q remains essentially the same as in YBCO. The relative importance of thermal and quantum fluctuations is measured by the ratio $\sqrt{G}/Q$ and using the usual expressions relating the penetration depth and the conductivity one finds

$$\frac{\sqrt{G}}{Q}\approx\frac{1}{2\sqrt{2}\pi^2}\frac{dl}{\varepsilon\xi^2(0)}. \tag{32}$$

III. QUANTUM STATISTICAL MECHANICS

We now can make use of the result (29) for the free-energy density and calculate the thermodynamic properties of the vortex lattice. Here we concentrate on the specific-heat density $C_v=-T\partial^2 f/\partial T^2$ and on the magnetic "susceptibility" $\chi=B(1/4\pi-\partial^2 f/\partial B^2)$. In order to find the specific-heat density we use the result (29) in its single-vortex version [only the explicit temperature dependence in (29) is relevant here]. The specific heat is determined by the low-frequency part of the spectrum with $\hbar\omega<T$, such that dispersive effects are irrelevant at low temperatures. For the dissipative case ($\alpha_l=0$) we obtain

$$C_v\approx\frac{4}{\pi^2}\frac{TB\eta_l}{\hbar\Phi_0}\int_0^\infty dx\frac{x^2}{\sinh^2 x}\int_{K_{BZ}/\varepsilon}^{k_\infty}\frac{dk_z}{\varepsilon_l(k_z)k_z^2}, \tag{33}$$

where $k_\infty\simeq 1/\max(d,\varepsilon\xi)$ and the lower cutoff in the k_z integral is provided by the bulk elastic modes. In the continuous anisotropic limit the relevant line tension is

$$\varepsilon_l(K_{BZ}/\varepsilon)\approx(\varepsilon^2\varepsilon_0/2)\ln(B_{cr}/B)$$

with $B_{cr}\approx H_{c2}$ and we obtain the final result

$$C_v\approx\frac{2\sqrt{\pi}}{3}\frac{1}{\varepsilon a_0^3}\frac{1}{\ln(B_{cr}/B)}\frac{T}{T_\odot^\eta}. \tag{34}$$

The analogue of the Debye temperature $T_\odot^\eta$ is given by the thermal time $t_{th}=\eta/c_{66}K_{BZ}^2$ of the overdamped vortex motion

$$T_\odot^\eta=\frac{\hbar}{t_{th}}=\frac{Q}{\sqrt{2G}}\frac{d\xi(0)}{\varepsilon a_0^2}T_c\approx 2\left[\frac{\pi\xi(0)}{a_0}\right]^2\frac{\xi(0)}{l}T_c. \tag{35}$$

Taking the parameters for YBCO and choosing a field $B\sim 1$ T the temperature scale takes the value $T_\odot^\eta\approx 10^{-3}T_c$. In strongly layered superconductors the fluctuations change their character at the crossover field

$$B_{cr}=B_{2D}\approx\pi\Phi_0\frac{\varepsilon^2}{d^2}\ln\frac{d}{\varepsilon\xi} \tag{36}$$

and the result (34) only applies to the low-field regime $B<B_{cr}$, where the vortices retain their line nature. For large magnetic fields $B>B_{cr}$ the vortex specific heat has been calculated by Bulaevskii and Maley[16] and we quote their result

$$C_v\approx\frac{5\pi}{12}\frac{1}{da_0^2}\ln\left[\frac{B}{B_{2D}}\right]\frac{T}{T_\odot^\eta}. \tag{37}$$

Using parameters typical for BiSCCO we obtain $B_{2D}\simeq 0.1-1$ T. Note the different field dependence $\propto\sqrt{B}/\ln B$ and $\propto\ln B$ for the results (34) and (37). The temperature dependence is given by the product $Tl(T)$, where the mean free path is expected to increase with decreasing temperature, $l\propto 1/T$, from simple high-temperature extrapolation, and to saturate at a finite value at low temperatures, producing a linear-in-T behavior for the specific heat.

An interesting situation arises in the superclean limit where the Hall term dominates the dynamics of the vortices. In this case the overdamped vortex motion changes to a Hamiltonian one and the interacting-vortex system develops propagating modes, the analogue of the phonon modes in the usual crystalline solid. These modes are the analogue of the Tkachenko waves,[35–37] which are the eigenmodes developed by the vortex system in uncharged superfluids where the vortex motion is dominated by the Hall term. The normal modes are easily obtained from the equation of motion

$$[-i\omega\alpha\mathbf{1}_\perp+\Phi(\mathbf{k})]\mathbf{u}(\mathbf{k})=0, \tag{38}$$

where Φ denotes the elastic matrix of the vortex system.[2] For the superclean limit the Hall term $-i\omega\alpha\mathbf{1}_\perp$ replaces the more familiar dissipative term $-i\omega\eta\mathbf{1}$. The latter produces the overdamped longitudinal and transverse modes $i\omega_L=\varepsilon_L/\eta$ and $i\omega_T=\varepsilon_T/\eta$, whereas we obtain the propagating modes

$$\omega=\sqrt{\varepsilon_L\varepsilon_T}/\alpha \tag{39}$$

for the Hamiltonian case (38). The transverse Hall force

mixes the longitudinal and transverse components,

$$\frac{u_x}{u_y}=\frac{i\sqrt{\varepsilon_L\varepsilon_T}K^2+(\varepsilon_L-\varepsilon_T)K_xK_y}{\varepsilon_LK_x^2+\varepsilon_TK_y^2} . \tag{40}$$

In the single-vortex limit we have $\varepsilon_L=\varepsilon_T$ and $u_x/u_y=i$. The dispersion of the Tkachenko waves is quadratic for the $K\rightarrow 0$ bulk modes and turns linear for $K>1/\lambda$ due to the dispersion in $c_{11}(\mathbf{k})$. In the single-vortex regime the dispersion is again quadratic, $\hbar\omega\simeq(\varepsilon_0\varepsilon^2/\pi n)k_z^2$ for the continuous anisotropic situation relevant for YBCO (here we concentrate on this material where experimental evidence for the realization of the superclean limit exists[38]). In the limit of zero dispersion the free energy (29) simplifies to

$$f=T\int\frac{dk_z}{2\pi}\int_{\mathrm{BZ}}\frac{d^2K}{(2\pi)^2}\ln\left[2\sinh\frac{\hbar\sqrt{\varepsilon_L\varepsilon_T}}{2\alpha T}\right] \tag{41}$$

and the general expression for the specific heat takes the form

$$C_v=\int\frac{dk_z}{2\pi}\int_{\mathrm{BZ}}\frac{d^2K}{(2\pi)^2}\left[\frac{\hbar\sqrt{\varepsilon_L\varepsilon_T}}{2\alpha T}\right]^2\sinh^{-2}\frac{\hbar\sqrt{\varepsilon_L\varepsilon_T}}{2\alpha T} . \tag{42}$$

With $C_v\propto T^{d/n}$, where d is the dimensionality of the system and n the exponent characterizing the dispersion $\omega\propto k^n$, we obtain the following qualitative behavior for C_v. At extremely low temperatures the bulk modes dominate and with $d=3,n=2$ we obtain $C_v\propto T^{3/2}$. With increasing temperature the dispersion in the elastic moduli becomes relevant and we enter a complicated crossover regime. Only at temperatures $T\gtrsim(d/\varepsilon a_0)^2T_\Theta$ does the situation simplify again when the single-vortex modes start to dominate and we obtain $(d=1,n=2)$

$$C_v=\frac{1}{a_0^2d}\left[\frac{T}{T_\Theta}\right]^{1/2}\int_0^{\sqrt{T_\Theta/T}}dy\frac{y^2}{\sinh^2y} , \tag{43}$$

with the analogue of the Debye temperature for the vortex system

$$T_\Theta=\frac{\pi}{2}\frac{\varepsilon_0\varepsilon^2}{d^2n}\approx\frac{\pi}{8\sqrt{2}}\frac{\varepsilon}{\sqrt{G}}\frac{T_c}{\xi(0)d^2n}\approx 0.2T_c \tag{44}$$

and where we have inserted parameters appropriate for YBCO in the last equation. Finally, for $T>T_\Theta$ we enter the classical regime where all the modes are excited and we find the classical limit $C_v=1/a_0^2d$.

The vortex translational specific heat calculated here competes with various contributions, e.g., the one due to the normal cores,[26] which is linear both in temperature T $(>\hbar\omega_0)$ and in the field B,

$$C_{vc}\simeq(K_F^2/d)(T/\varepsilon_F)(B/H_{c2}) ,$$

or the one due to the phonons $C_{vp}\simeq(K_D^2/d)(T/\Theta_D)^3$, where K_D and Θ_D denote the planar Debye wave vector and the Debye temperature, respectively. The relative contribution of the various terms can easily be obtained by comparing the relevant volume per degree of freedom and the temperature scale involved, e.g., the comparison between the vortex contribution for the Hamiltonian case and the phonon contribution involves the small parameter a/a_0, where a is the lattice constant of the crystal.

Second, we turn to the reversible magnetic properties. Here we concentrate on the low-temperature limit, where we can replace the summation over Matsubara frequencies by a simple integration. It is then convenient to go back to the partition function (28) and find the appropriate expression for the $T=0$ free-energy density f. The fluctuation contribution to the magnetization is determined by the high-frequency part of the spectrum, allowing us to drop the Hall term and to use the high-frequency limit $\eta(\omega_n)\approx\eta(0)/|\omega_n|\tau$ for the friction coefficient. The factors appearing in the product in (28) reduce to a set of undamped harmonic-oscillator modes with frequencies $[(\varepsilon_{(L)T}+\eta(0)/\tau_r)/\mu]^{1/2}$. Replacing the sum over Matsubara frequencies by a simple frequency integration we obtain

$$f=\int\frac{dk_z}{2\pi}\int\frac{d^2K}{(2\pi)^2}\frac{\hbar}{2}\left\{\left[\frac{1}{\mu}\left[\varepsilon_L+\frac{\eta(0)}{\tau_r}\right]\right]+\left[\frac{1}{\mu}\left[\varepsilon_T+\frac{\eta(0)}{\tau_r}\right]\right]\right\} . \tag{45}$$

The frequency integral has effectively been cut off by the mass term $\mu\omega_n^2$ and we take a closer look at the possible origin of such a term. A well-known contribution to the vortex mass is of electromagnetic origin[39] producing a mass $\mu_l^{\mathrm{em}}\approx(\Phi_0/4\pi c\xi)^2$. The corresponding cutoff frequency $\hbar\Omega\approx\hbar\sqrt{\eta_l/\mu_l\tau_r}\simeq\hbar c/\lambda$ then is of the order of 10^4 K. A second contribution to the vortex mass is due to strain fields induced by the vortex,[40,41] generating a vortex mass μ_l^{sf} which is of the same order as that produced by the electromagnetic coupling. The frequency cutoff produced by the vortex mass then turns out to be rather high, beyond the regime of applicability of the transport coefficients as given by (19). We should expect that at frequencies matching the energy gap of the superconductor the vortex motion is highly dissipative due to the creation of quasiparticles and a reasonable cutoff on the frequency integral in the free-energy density f then is given by the gap energy, $\hbar\Omega\sim 2\Delta$. Below we will treat the cutoff $\hbar\Omega=\nu\Delta$ as a parameter when we compare our results to experimental observations. It is then convenient to introduce the dimensionless expression.

$$\Omega\tau_rQ\approx\frac{\nu}{\xi K_F} , \tag{46}$$

with ν serving as the remaining fitting parameter in the comparison to various experiments [with $n\approx 2.5\times 10^{21}$ cm^{-3} we obtain $K_F\approx 0.15$–0.2 Å^{-1}; note that in (46) the temperature dependencies of τ_r and Q are canceled out].

Let us go on and perform the integration over the various $\mathbf{k}$ modes in (45). For a strongly layered material the tilt modes are very soft and the longitudinal and transverse elastic modes (27) are dominated by the compression and shear energies. We thus can use the approximations $\varepsilon_L\approx B^2/4\pi\lambda^2$ and $\varepsilon_T\approx(B^2/16\pi\lambda^2)K^2/K_{\mathrm{BZ}}^2$, which

properly account for the dispersive effects. The integrations in (45) are restricted to the regions $|k_z|<\pi/d$ and $K^2<K_{BZ}^2$. Finally, the magnetization M is given by the thermodynamic relation $M=B/4\pi-\partial f/\partial B$ and we obtain the fluctuation contribution

$$M=\frac{\Phi_0}{32\pi^2\lambda^2}\ln\frac{\alpha B}{H_{c2}} -\frac{\Phi_0}{4\pi^2\lambda^2}\frac{\nu}{\xi K_F}\left[\frac{1+\frac{3}{2}B/B_Q}{(1+B/B_Q)^{1/2}}+\left[1+\frac{B}{4B_Q}\right]^{1/2}\right], \tag{47}$$

where

$$B_Q=\frac{4\pi\lambda^2}{\Phi_0}\frac{\eta_l}{\tau_r}\simeq H_{c2}\ . \tag{48}$$

The experimentally measured susceptibility takes the form

$$\chi=\frac{\partial M}{\partial\ln B} =\frac{\Phi_0}{32\pi^2\lambda^2}-\frac{\Phi_0}{16\pi^2\lambda^2}\frac{\nu}{\xi K_F}\frac{B}{B_Q}\left[\frac{4+3B/B_Q}{(1+B/B_Q)^{3/2}}+\frac{1}{(4+B/B_Q)^{1/2}}\right] \tag{49}$$

and we find that quantum fluctuations tend to suppress the magnetic susceptibility at large fields. Recent measurements of the (low-temperature; $T=35$ K) reversible magnetization in BiSCCO single crystals[17] show a marked decrease of the magnetic "susceptibility" χ with increasing magnetic field, amounting to $\sim 50\%$ of the mean-field value at fields of the order of 7 T (see Fig. 1). These findings are in general agreement with the result (49) if we choose $\nu\approx 2.5$, producing a cutoff frequency $\hbar\Omega$ of the order of the gap energy. Note that additional mean-field-type corrections due to the finite extent of the vortex cores also produce a decrease in the susceptibility with increasing magnetic field.[42] In our analysis (Fig. 1) we have taken this effect into account and have found that, while it does contribute to the suppression of the diamagnetic response, it cannot explain the experimentally measured suppression of χ.

Comparing our results with those of Bulaevskii *et al.*,[17] the main difference is found in the treatment of the vortex dynamics. Whereas in our approach we account for dispersive effects (and consequently have to deal with a *linear* divergence in the frequency summation), Bulaevskii *et al.* base their calculations on a nondispersive friction coefficient (resulting in a mere *logarithmic* divergence in the frequency summation). As a result, the frequency cutoff poses less of a problem in the approach of Bulaevskii *et al.* On the other hand, it seems that a consistent explanation of various experiments (quantum creep, diamagnetic response) relies on taking these dispersive effects into account. Indeed, the expression for the quantum parameter Q used in (46) is identical to the expression used in the description of quantum creep at low temperatures, where the theoretical results compare favorably with experimental data[43,44] if we use for ρ_N the normal-state resistivity extrapolated from high temperatures. Furthermore, this approach is in agreement with measurements of the flux-flow resistivity by Kunchur, Christen, and Phillips[45] who find a Bardeen-Stephen result with ρ_N extrapolated from high temperatures. A rather large value for the sheet resistivity (close to the quantum limit, $\rho_N/d\approx e^2/\hbar$) has to be assumed[17] in order to explain the experimental data on the basis of nondispersive transport coefficients.

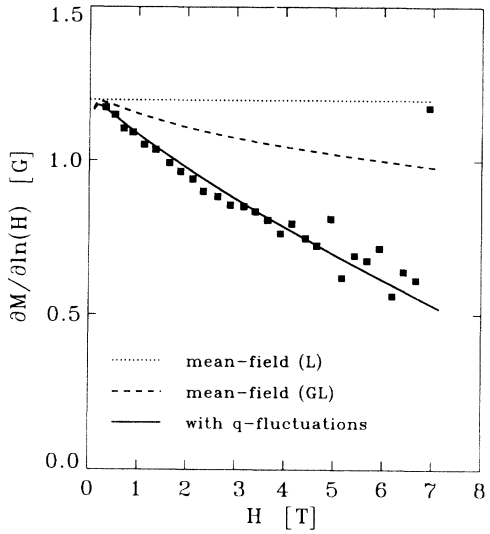

FIG. 1. Diamagnetic "susceptibility" $\chi=\partial M/\partial\ln H$ versus magnetic field for a BiSCCO single crystal at $T\approx 35$ K. The data (solid squares) are from Bulaevskii *et al.* (Ref. 17). The dotted line is the mean-field London result. Including corrections due to the vortex cores (Ref. 42) leads to a reduction of χ with increasing field ($\approx 15\%$ at 7 T). Including the effect of (quantum) fluctuations we can account for the data if we choose the parameter $\nu\approx 2.5$, which is consistent with theoretical expectations and with other experimental findings (quantum creep, melting).

IV. VORTEX-LATTICE MELTING

Various analytical and numerical methods have been applied to the problem of vortex-lattice melting,[3–5,46–50] particularly in view of application to the high-temperature superconductors. A very simple and direct approach to the melting phenomenon is given by the Lindemann criterion,[51] stating that the lattice melts when the mean displacement amplitude $\langle u^2\rangle^{1/2}$ of the lattice constituents reaches a fraction $c_L<1$ of the lattice constant a_0,

$$\langle u^2\rangle\Big|_{T=T_m}=c_L^2 a_0^2\ . \tag{50}$$

For the vortex lattice we have $a_0\approx(\Phi_0/B)^{1/2}$ and the

Lindemann number c_L typically[48] is in the range $c_L \approx 0.1-0.3$. The quantum corrections to the mean squared displacement field $\langle u^2 \rangle_{\rm th}$ are again dominated by large frequencies and we can drop the Hall term in the action. The mean squared displacement amplitude $\langle u^2 \rangle$ comprising both thermal and quantum fluctuations of the vortices then is given by

$$\langle u^2 \rangle = \frac{\int \mathcal{D}[\mathbf{u}] \sum_n |\mathbf{u}_n|^2 \exp\{-\mathcal{S}[\mathbf{u}]/\hbar\}}{\int \mathcal{D}[\mathbf{u}] \exp\{-\mathcal{S}[\mathbf{u}]/\hbar\}} \tag{51}$$

$$\simeq T \sum_n \int \frac{d^3k}{(2\pi)^3} \frac{1}{\eta(\omega_n)|\omega_n| + c_{66}K^2 + c_{44}(\mathbf{k})k_z^2} + \frac{1}{\eta(\omega_n)|\omega_n| + c_{11}(\mathbf{k})K^2 + c_{44}(\mathbf{k})k_z^2} . \tag{52}$$

The $n=0$ term produces the well-known thermal contribution and a simple estimate is given by the expression

$$\langle u^2 \rangle_{\rm th} \approx \frac{T a_0}{\sqrt{\pi \varepsilon \varepsilon_0}} \approx \left[\frac{G}{\beta_{\rm th}} \right]^{1/2} \frac{\sqrt{b}\, t}{1-t-b} a_0^2 , \tag{53}$$

which becomes large in the oxide superconductors due to the large value of the Ginzburg number G. Here, $b = B/H_{c2}(0)$ and $t = T/T_c$ denote the scaled magnetic field and temperature and $\beta_{\rm th} \approx 2.5$. Also, we have taken the suppression of the order parameter close to the upper critical field into account, leading to an increase in the screening length $\lambda^2 \to \lambda'^2 = \lambda^2/[1-b/(1-t)]$.[22] This correction factor becomes important at low temperatures and high magnetic fields and shifts the melting line towards smaller field values; see the discussion below. Note that the $\mathbf{K}$ integration for the thermal component is dominated by the Brillouin-zone boundary and the relevant k_z modes are determined by the competition between the shear and the tilt energy, $k_z \simeq \pi/\varepsilon a_0$. A more careful calculation[5] gives the result

$$\langle u^2 \rangle_{\rm th} \approx \frac{\sqrt{G}}{\sqrt{3}\pi} \frac{\sqrt{b}\, t}{1-t} \frac{1}{1-b/(1-t)} \times \left[\frac{4(\sqrt{2}-1)}{[1-b/(1-t)]^{1/2}} + 1 \right] a_0^2 , \tag{54}$$

which mainly changes the numerical parameter $\beta_{\rm th} \approx 5.6$ in (53).

The quantum contribution $\langle u^2 \rangle_q$ is determined by the remaining terms in (51) with $n \neq 0$. The integral is again dominated by the large $\mathbf{K}$ values near the Brillouin-zone boundary where $c_{11}(K_{\rm BZ}) \simeq c_{66}$; hence the transverse and longitudinal modes contribute with similar weights. Here, we concentrate on the continuous anisotropic case (YBCO), where the elastic energy is dominated by the single-vortex contribution, i.e.,

$$c_{66}K^2 + c_{44}(K_{\rm BZ})k_z^2 \to \frac{\varepsilon_l(k_z)}{a_0^2} k_z^2 \simeq \frac{\varepsilon^2 \varepsilon_0}{a_0^2} k_z^2 . \tag{55}$$

The (single-vortex) elastic energy competes with the dynamic term $\eta(\omega_n)|\omega_n|$ and we find

$$\langle u^2 \rangle_q \approx \frac{4}{\pi} \frac{T}{\varepsilon} \sum_{n>0} \frac{1}{\sqrt{\eta_l |\omega_n| \varepsilon_0}} \arctan \frac{\pi \varepsilon}{d} \left[\frac{\varepsilon_0}{\eta_l |\omega_n|} \right]^{1/2} . \tag{56}$$

With $\sqrt{\varepsilon_0/\eta_l|\omega_n|} < \xi/\sqrt{2}$ we can expand the last factor in (56) and obtain

$$\langle u^2 \rangle_q \approx \frac{4T}{d} \sum_{n>0} \frac{1}{\eta_l(\omega_n)|\omega_n|} . \tag{57}$$

Note that in (57) the k_z integration equally weights all of the allowed range $2\pi/d$, whereas $k_z \simeq \pi/\varepsilon a_0$ are the relevant modes in the thermal part (53). Again, the summation over Matsubara frequencies has to be cut off at high frequencies $\omega_n \approx \Omega \sim \nu\Delta/\hbar$ and hence the number of terms $N \simeq \hbar\Omega/2\pi T$ contributing to the frequency summation in (57) is of the order unity. The final result for the quantum part of the displacement amplitude takes the form

$$\langle u^2 \rangle_q \approx \frac{4}{\pi^2} Q \Omega \tau_r \xi^2 \approx \frac{4\nu}{\pi^2} \frac{\xi}{K_F} . \tag{58}$$

The quantum contribution $\langle u^2 \rangle_q$ is independent of the magnetic field and using parameters appropriate for YBCO we can estimate its magnitude to be of the order of ξ^2.

The final step in the determination of the melting line is the application of the Lindemann criterion to the displacement amplitude $\langle u^2 \rangle^{1/2}$. The important question then is whether the (quantum) smearing of the vortex core as determined above can be felt by the neighboring vortices and thus becomes relevant for the melting transition or not. For the finite-frequency response relevant here we have to base our discussion on the time-dependent Ginzburg-Landau theory.[52,53] The motion of the vortices sets up screening currents which involve both a quasiparticle (j_N) and a London contribution (j_L),

$$\mathbf{j} = \sigma_N(\omega_n) \left[-\frac{|\omega_n|}{c} \mathbf{Q} - \nabla \Phi \right] - \frac{c}{4\pi\lambda^2} \Delta^2 \mathbf{Q} . \tag{59}$$

The transverse component of this current decays on the length scale λ, the screening length for the transverse component of the gauge-invariant vector potential $\mathbf{Q} = \mathbf{A} - (\Phi_0/2\pi)\nabla\chi$, whereas the longitudinal part is screened on the charge imbalance length[54,55] $l_E \sim \xi(0)$, the screening length of the gauge-invariant scalar potential $\Phi = \phi + (\Phi_0/2\pi c)\partial_t \chi$. The ratio of the two current densities is given by

$$\frac{j_N}{j_L} = \frac{4\pi\lambda^2 \sigma_N(\omega_n)|\omega_n|}{c^2} \sim \frac{|\omega_n|\tau_r}{1+|\omega_n|\tau_r} \frac{1}{\Delta^2(T)} . \tag{60}$$

For vanishing frequencies (e.g., for the thermal component of $\langle u^2 \rangle$) the response is always dominated by the London current density j_L and vortices within the screening length λ are mutually affected by their motion (see Fig. 2); on the other hand, for high frequencies the London currents are relevant only at low temperatures and

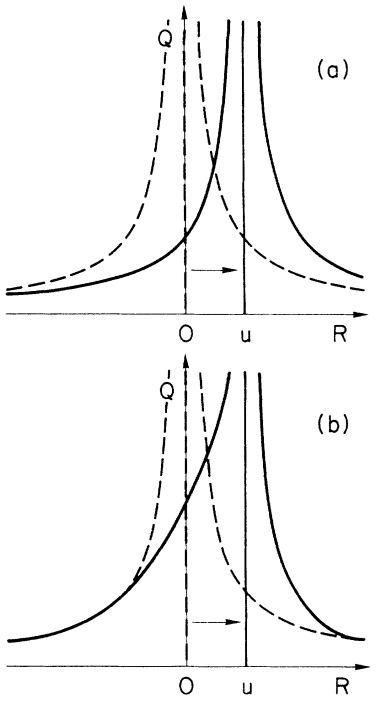

FIG. 2. Dynamical response of the supercurrent flow ($\propto \mathbf{Q}$) encircling a moving vortex. (a) For temperatures away from the transition the supercurrent is able to follow the motion of the vortex. (b) At temperatures close to the transition the vortex fluctuations are screened at a short distance due to the normal current flow driven by the scalar potential in the core region.

the normal current density j_N becomes dominant close to T_c. In the latter case the motion of the vortex cores is screened by the normal current flow around the core (the relevant scale is the charge imbalance length l_E) and the neighboring vortices are not affected. Hence we conclude that the quantum motion of the vortices can be felt by the neighbors, and thus is relevant for the melting transition, only at temperatures away from the transition, where the superconducting order parameter has become appreciable. Related to this problem is the question of the dissipation close to T_c. Assume, contrary to the above argumentation, that the vortex motion remains coupled to the London currents upon approaching T_c. We then can express the vector potential $\mathbf{Q}$ through the vortex displacement $\mathbf{u}$, $\mathbf{Q} \simeq -(\mathbf{u}\cdot\nabla)\mathbf{Q}_0 \sim u\Phi_0/R^2$, where $\mathbf{Q}_0 = -\Phi_0 \hat{\mathbf{z}} \times \hat{\mathbf{R}}/2\pi R$ is the vector potential set up by a static vortex. The dissipation produced by the normal currents $j_N = -\sigma_N(\omega_n)|\omega_n|\mathbf{Q}$ flowing outside the core region ($R > l_E$) is given by $\sigma_N E^2 \sim \sigma_N \Phi_0^2 u^2 \omega_n^2 / R^4 c^2$, which upon integration over $R > l_E$ gives the result $P \sim \sigma_N \Phi_0^2 u^2 \omega_n^2 / l_E^2 c^2$ for the dissipated power. The nonvanishing of P on approaching T_c then is due to our wrong assumption that the vortex motion is still coupled to the London currents close to T_c. Hence, close to T_c the vortex motion is screened by normal currents on the length scale l_E and the transverse component of the vector potential (which drives the London currents) remains unaffected.

A second remark concerns the form (58) of the quantum component of the displacement field. Whereas the thermal component explicitly contains the shear modulus the quantum component does not. The reason for this difference is easily understood by noting that the thermal fluctuation amplitude is determined by the potential of the other vortices, whereas (within the present approximation) the quantum amplitude is determined by the dynamical term alone. Nevertheless, the quantum fluctuations also add to the smoothing of the intervortex potential and thereby to the reduction of the shear modulus which ultimately leads to the melting of the vortex lattice.

From the above discussion we conclude that away from the transition temperature T_c both thermal and quantum contributions do contribute to the melting transition of the vortex lattice; however, due to their different nature with different weights in general. Straightforward application of the Lindemann criterion then is, strictly speaking, only possible at $T=0$, where the transition is purely quantum, or at high temperature, where it is purely classical, whereas in the intermediate regime a weighted sum of the static and the dynamic components is more appropriate. Here we ignore this complication and take a simplified approach invoking only one Lindemann number for both quantum and classical contributions. Combining (53) and (58) with equal weights and using the Lindemann criterion (50) we have to solve the following equation for the melting line $b_m(t)$,

$$\frac{\langle u^2 \rangle}{a_0^2} \approx \left[\frac{G}{\beta_{\rm th}}\right]^{1/2} \frac{\sqrt{b}}{1-t-b}\{t + q\sqrt{b}\,[1-b/(1-t)]\} \approx c_L^2 , \tag{61}$$

with

$$q = \frac{2\sqrt{\beta_{\rm th}}}{\pi^3}\frac{Q}{\sqrt{G}}\Omega\tau_r \approx 2.4\frac{\nu}{K_F\xi} . \tag{62}$$

The terms up to linear order in $\sqrt{b}$ produce the well-known high-temperature form $b_m \propto (1-t)^2/t^2$ for the melting line. The terms linear in b account for the suppression of the order parameter close to H_{c2} and for the quantum contributions to $\langle u^2 \rangle$. The term of order b^2 accounts for the mixing of the latter two corrections. Neglecting this higher-order term we can solve for b and obtain a compact result for the new shape of the melting line

$$b_m = \frac{4\theta^2}{(1+\sqrt{1+4S\theta/t})^2} , \tag{63}$$

with the temperature variable

$$\theta = c_L^2 \left[\frac{\beta_{\rm th}}{G}\right]^{1/2}\left[\frac{T_c}{T}-1\right] \tag{64}$$

and the suppression parameter S

$$S = q + c_L^2 \left[\frac{\beta_{\rm th}}{G}\right]^{1/2} . \tag{65}$$

The main features of the result (63) are the following. (i) Taking into account both the order-parameter suppression close to H_{c2} as well as quantum fluctuations of the vortices in the determination of the melting transition leads to a shift of the melting line towards smaller temperatures and fields, and (ii) the form of the melting line cannot be expressed via a simple power law in $(1-T/T_c)$ but adopts the more complicated dependence given by (63). In the limit $\theta \to 0$ the simple thermal result $b \propto (1-t)^2$ is recovered, whereas a linear dependence on θ is obtained at low temperatures,

$$b_m \approx \begin{cases} \theta^2, & \theta \to 0 \\ \dfrac{\theta t}{S}, & \theta > \dfrac{1}{S}. \end{cases} \tag{66}$$

The effects of quantum fluctuations thus become important at temperatures away from T_c and for large magnetic fields H. In a more accurate analysis we should use for the thermal component the result of Houghton, Pelcovits, and Sudbø[5] as given by (54) and solve the resulting equation self-consistently. In fact, this will be the approach taken below when comparing the present theoretical results with experimental data. However, no closed expression for the melting line can be obtained in this case.

In order to compare our theoretical results with experiments we proceed in two steps. We first discuss the accuracy of the various available theoretical results in comparison with the experimental data on the melting line as measured via a resistive technique[18] on a very clean YBCO single crystal. Second we will compare our line shape with available data on the melting line for different materials and measured with different techniques.

The observation of a sharp resistive transition in a very clean untwinned single crystal of YBCO provides strong evidence for the existence of a first-order melting transition.[7] A sharp first-order melting line up to fields of 10 T and followed by a continuous transition at even higher field values $10 < B < 16$ T has been observed[18] recently in such a clean crystal. Choosing the parameters $\lambda(0), \xi(0), \varepsilon$, and ρ_N as cited above we have $G \approx 4 \times 10^{-3}$ and $Q \approx 0.2$. The remaining adjustable parameters are the Lindemann number c_L (required to lie within the range 0.1–0.3) and the parameter ν determining the cutoff frequency Ω; see (46). Note that within our approach the upper critical field $H_{c2}(0)$ is not a free parameter: Combining the measured[56,57] slope $dH_{c2}/dT \approx -1.9$ T/K with the value $T_c \approx 90$ K we obtain an extrapolated upper critical field $H_{c2}(0) \approx 170$ T. Figure 3 shows a simple $(T_c/T-1)^2$ fit, valid close to T_c, as well as the more elaborated thermal result obtained by Houghton, Pelcovits, and Sudbø[5] calculated on the basis of (54). In both cases a Lindemann number $c_L \approx 0.27$ has been used as an optimal fit parameter. As expected the more accurate result by Houghton, Pelcovits, and Sudbø shifts the melting line towards smaller temperatures and fields. As the data extend up to 20 K below the transition we had to correct the $(1-t)$ dependence in (54) by the more accurate expression $(1-t^2)/2$, thus accounting for the deviation from the simple $1-t$ Ginzburg-Landau temperature dependence valid only close to T_c. Also, we have used a transition temperature $T_c \approx 90.5$, which is within the G region of the value $T_c \approx 90.0$ quoted in Ref. 18. With these measures an optimal fit is obtained providing satisfactory agreement with the data below a field of ~ 3 T. Combining the thermal result by Houghton, Pelcovits, and Sudbø (54) with the quantum corrections (58) into a Lindemann criterion and solving the resulting equation numerically, very good agreement with the experimental data is obtained within the entire field range up to 10 T if we choose a Lindemann number $c_L \approx 0.30$ and take for

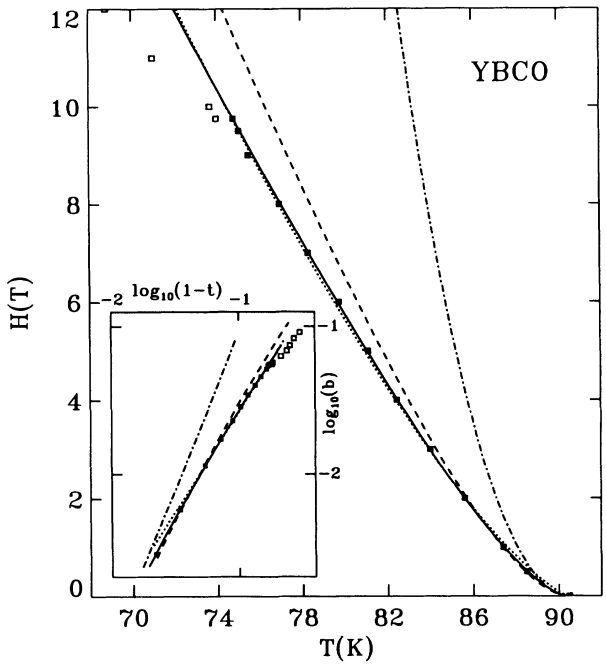

FIG. 3. Melting lines calculated via the Lindemann criterion. The result of different degrees of accuracy in the theoretical treatment is shown and compared with the shape of the melting line as obtained by Safar *et al.* (Ref. 18) (the solid symbols mark a sharp first-order transition, whereas the open symbols refer to the continuous transition observed at higher magnetic fields $B > 10$ T). The mean-field transition temperature was chosen $T_c \approx 90.5$. The thermal power-law behavior $B_m \propto (T_c/T-1)^2$ has a very limited range of applicability (dash-dotted line). The more elaborate result by Houghton, Pelcovits, and Sudbø (Ref. 5) takes the renormalization of the elastic coefficients close to the upper critical field line into account and leads to a considerable improvement (dashed line; the Lindemann number $c_L = 0.27$ has been chosen such as to provide a good fit to the high-temperature data). The shape for the melting line which additionally accounts for quantum fluctuations gives very good agreement over the entire field range if we choose a Lindemann number $c_L \approx 0.30$ and take $\nu \approx 4$ (solid line). The crossover to a continuous transition at high fields ($B > 10$ T) lies outside the realm of the present description, which ignores the effects of disorder. Finally, a simple power-law fit $B_m \propto (1-T/T_c)^\alpha$ gives an exponent $\alpha \approx 1.35$ (dotted line). Note, however, that this power-law form lacks any theoretical basis and represents only a fitting ansatz. The inset shows all four curves in a double-logarithmic representation.

the parameter $\nu \approx 4$. A value $c_L \approx 0.3$ for the Lindemann number has also been obtained for the quantum melting transition in a Wigner crystal by Ceperley.[58] We note that the simplified (closed-form) result (63) with the two parameters c_L and q already provides a good fit to the melting line. The changeover from a first-order melting to a continuous glass transition observed in this crystal[18] and taking place at a field $B \approx 10$ T suggests that the effect of disorder becomes more important in the high-field–low-temperature regime. Note that the crossover to the glass transition at high fields is outside the realm of the present description.

In our previous work[15] the suppression of the order parameter close to the upper critical field line was neglected. This led us to overestimate the effect of quantum fluctuations on the melting line in YBCO. In fact, only part of the suppression parameter S appearing in (63) can be attributed to the effect of quantum fluctuations, whereas the larger contribution to S actually arises from the suppression of the order parameter.

In the past it has become common[59,8,60,61,20] to fit the form of the irreversibility or melting line in terms of a simple power law in $1-T/T_c$. One should note, however, that the ansatz $B_m(T) \propto (1-T/T_c)^{\alpha}$ lacks any theoretical background and even the most simple thermal result already exhibits a different temperature dependence. Nevertheless, one can argue that close to T_c such an ansatz (with $\alpha=2$) should capture the main temperature dependence of the melting line and this is actually the case; however, the range where a satisfactory agreement with the experimental data can be obtained is only a few kelvin wide (the situation is better for the BiSCCO material; see below). Somewhat surprisingly, taking α as a fit parameter good agreement is obtained between the simple power-law form $B_m(T) \propto (1-T/T_c)^{\alpha}$ and the data over the entire experimental temperature range (see Fig. 3). For the above example[18] the optimal power-law fit is obtained by choosing $\alpha \approx 1.35$. The arbitrariness in this fitting procedure, however, becomes clear when noting that an equally good agreement with the data can be obtained if one uses the variable $(1-t^2)/2t$ instead of $1-t$; in this case the optimal exponent has to be changed to $\alpha \approx 1.22$.

The crossover between the thermal- and the quantum-dominated melting transition takes place at the reduced field $b_q \approx 1/q^2$. Using the value $H_{c2}(0) \approx 170$ T and $q \approx 4$ (i.e., $\nu \approx 4$) as extracted from the above comparison with the experimental data we obtain a crossover field $B_q \approx 10$ T. For large fields $B > B_q$ the transition is dominated by quantum fluctuations and the resulting high-temperature phase is a vortex quantum liquid. Making use of the above analysis we can rewrite the mean squared displacement field in the simple form

$$\langle u^2 \rangle \approx \xi^2 \left[\frac{2.2}{\sqrt{B}} + 0.7 \right], \tag{67}$$

with the field B measured in tesla. Quantum fluctuations smear the vortex core over a distance which is roughly equal to the spatial extent of the vortex core itself.

Due to the competition between thermal and quantum fluctuations the high-temperature superconductors are not the best candidates for the observation of a quantum melting transition and for the realization of a quantum vortex liquid. Quantum fluctuations become more relevant at low temperatures and high magnetic fields; hence, in order to realize a pure $T=0$ quantum transition, a conventional superconductor with a smaller upper critical field provides more favorable experimental conditions. Furthermore, quantum effects are enhanced by a high resistivity and a short cutoff in the quantum parameter Q; thus amorphous thin films close to the superconductor-insulator transition are in fact good candidates for the observation of a quantum melting transition and results have been reported recently for amorphous Nb_3Ge films.[62]

Second, we compare our theoretical result (63) with a variety of experiments determining the melting transition in other crystals and materials and based on different measuring techniques. In Fig. 4 we present a comparison with two more YBCO single crystals exhibiting the characteristics of a first-order melting transition.[7,19] Furthermore, we compare our line shape with the data of Schilling, Ott, and Wolf,[20] who have suggested an alternative procedure for an accurate determination of the irreversibility line based on magnetometry in the static limit and who have applied this method in their study of different materials such as YBCO (Fig. 5),[20] and BiSCCO (Fig. 6).[21] The parameters describing the individual melting lines are given in the figure captions. For YBCO we consistently find a Lindemann number $c_L \approx 0.25$–0.30 and a cutoff parameter $\nu \approx 4$. Concentrating next on the layered BiSCCO superconductors, we can apply the result (63) at low magnetic fields, $B < B_{2D}$ [see (36)], where the melting line still can be described within a three-dimensional (3D) anisotropic continuum elastic theory. For large fields $B > B_{2D}$ the fluctuations of the vortex lattice become two-dimensional in nature and the description of the vortex-lattice melting is better approximated by starting from a 2D dislocation-mediated Berezinskii-Kosterlitz-Thouless transition. Due to the very large anisotropy the value for the Ginzburg number G is greatly enhanced in BiSCCO as compared to YBCO, $G \approx 4$. Note that here the Ginzburg number G should be understood as a useful combination of parameters determining the strength of thermal fluctuations in the vortex lattice rather than the width of the critical regime. Whereas G is greatly enhanced by the strong layering, the quantum resistance Q remains essentially unchanged as compared to YBCO. The increased importance of the thermal over the quantum fluctuations in BiSCCO can be traced back to the different ways the relevant k_z fluctuation modes enter the formulas for the displacement amplitude. The quantum parameter q becomes vanishingly small and we cannot determine a value for ν. We obtain good agreement with the data of Schilling, Ott, and Wolf[21] within the field range $B \lesssim 0.1$ T if we choose a Lindemann number $c_L \approx 0.2$, the only remaining free parameter (see Fig. 5). The result $c_L \approx 0.2$ for the Lindemann number is in good agreement with the Monte Carlo simulations of the melting line by Ryu *et al.*[48] based on a model appropriate for BiSCCO. For larger values of the magnetic field

the two-dimensional nature of the material starts to manifest itself and our 3D result (63) cannot be applied. The approximate power-law fit gives the exponent $\alpha=2.5$. The exponent $\alpha>2$ can be understood by noting that the thermal result is roughly described by the dependence $[(1-t^2)/t]^2$ which differs from the simple power law $(1-t)^2$ as t drops far below T_c. Besides substituting the more accurate $(1-t^2)/2$ dependence for the simple $1-t$ dependence in (54), we have also used the renormalized value $T_R \approx 88$ K for the transition temperature[63,64] instead of the experimentally measured transition temperature $T_c \approx 84.5$ as the Ginzburg-Landau parameters extra-

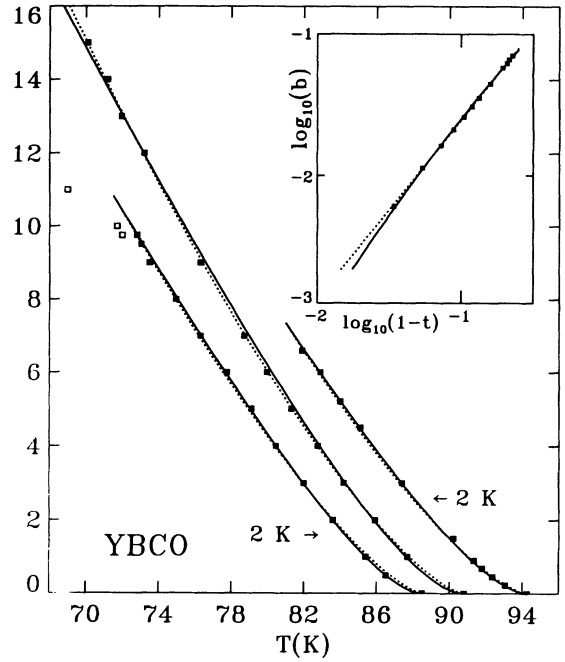

FIG. 4. Melting lines calculated via the Lindemann criterion taking quantum fluctuations into account (solid lines). The data points are the results as obtained by Safar and co-workers (Refs. 7, 18, and 19). The width of the symbols roughly corresponds to the experimental precision in the determination of the melting line based on the observation of a hysteretic trace in the resistivity. For the data of Ref. 7 the parameters are $T_c \approx 92.3$, $c_L \approx 0.29, \nu \approx 4$, and the power-law approximation (dotted lines) to the melting line is characterized by an exponent $\alpha \approx 1.4$. The data have been shifted by +2 K along the temperature axis. The parameters for the data showing both a first-order melting transition at low fields $B \lesssim 10$ T and a continuous phase transition (open squares) at high fields (Ref. 18) are $T_c \approx 90.5, c_L \approx 0.30, \nu \approx 4$, and the power-law approximation to the melting line provides the exponent $\alpha \approx 1.35$. The upper part of the melting line (open squares) is strongly influenced by the disorder and we cannot describe this effect within the present theoretical considerations. The data have been shifted by −2 K along the temperature axis. Finally, the data obtained from a very clean crystal (Ref. 19) (a $T_c \approx 90.8$ has been chosen) showing a hysteretic transition up to a field of 15 T are described by the following set of parameters: $c_L \approx 0.28, \nu \approx 3$, and $\alpha \approx 14$. The inset shows the corresponding data (Ref. 19) on a double-logarithmic scale. The parameter sets obtained for the different crystals are roughly consistent.

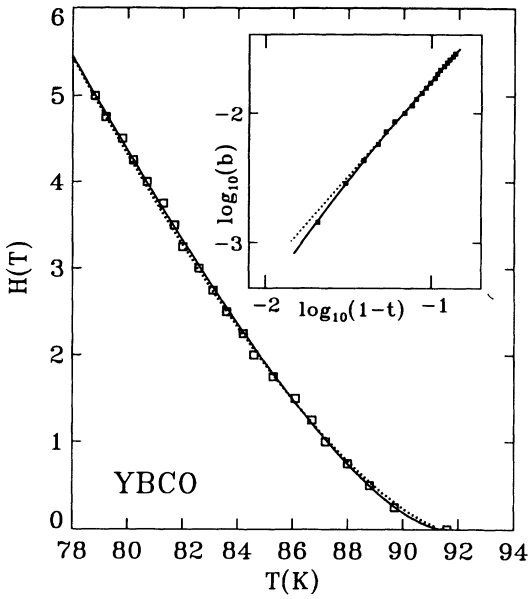

FIG. 5. Melting line calculated via the Lindemann criterion taking quantum fluctuations into account (solid line). The data points are the result obtained by Schilling, Ott, and Wolf (Ref. 20) for a YBCO single crystal ($T_c \approx 91.6$). The shape of the melting line is well described by the parameters $c_L \approx 0.25$ and $\nu \approx 4$. The dotted line is the approximate power-law fit $B_m \propto (1-T/T_c)^\alpha$ with $\alpha \approx 1.46$. The inset shows the same data within a double-logarithmic representation.

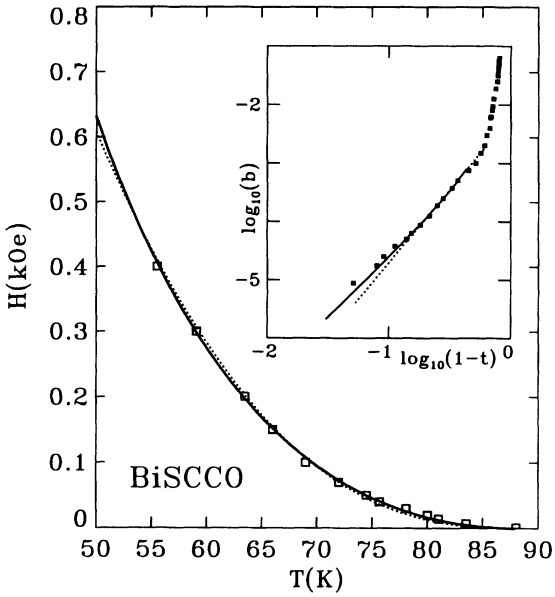

FIG. 6. Melting line determined via the Lindemann criterion (solid line) for a strongly layered BiSCCO single crystal. The data points are the result obtained by Schilling, Ott, and Wolf (Ref. 21) ($T_R \approx 88.0$). The shape of the melting line is dominated by thermal fluctuations and is well described by the single remaining parameter $c_L \approx 0.20$. Since quantum fluctuations are not important for this case, the parameter $\Omega\tau_r$ cannot be extracted. The dotted line is the approximate power-law fit with an exponent $\alpha=2.5$. The inset shows the same data in a double-logarithmic representation. For large magnetic fields $B > B_{2D}$ two-dimensional fluctuations become important. This high-field part of the melting line lies outside the region of applicability of the present 3D theory.

polate to T_R rather than to T_c (more precisely, T_R denotes the temperature where the fluctuation-corrected lower critical field line extrapolates to zero[64]). With these measures we obtain a very good agreement between the experimental data[21] and the thermal theory of Houghton, Pelcovits, and Sudbø[5] over a temperature range as large as ~ 40 K. This result has to be compared with the case of YBCO where the thermal theory cannot provide a satisfactory agreement over a temperature range more than 5 K wide. The difference between the anisotropic YBCO and the layered BiSCCO superconductors can be consistently explained by taking quantum corrections into account, which are predicted to be relevant for YBCO but not for BiSCCO.

The above analysis has been based on the assumption of a constant (i.e., field- and temperature-independent) Lindemann parameter c_L. Simple scaling arguments[2] valid for the thermal case in the London regime in fact do support this idea. However, even for the thermal case the regime where the London theory can be applied [i.e., where the suppression of the order parameter as described by the correction factors $1-b/(1-t)$ in (54) is irrelevant] is very limited: inspection of Fig. 3 shows this region to extend only a few K below T_c. The same analysis for the BiSCCO sample[21] shows that the London theory provides good results within a temperature region extending about 20 K below T_c. Within the Ginzburg-Landau region the suppression of the order parameter becomes relevant and the simple scaling arguments fail. Similarly, including quantum fluctuations we have to replace the free-energy functional by the Euclidean action which again does not exhibit the simple scaling of the London free energy. In this situation we can make some progress by referring to the Monte Carlo analysis of the melting transition in BiSCCO carried out by Ryu *et al.*,[48] from which one would expect c_L to increase slightly with field, implying an additional upward curvature of the melting line. Transferring this result to the case of YBCO (Fig. 3), one then would expect the quantum fluctuations to play an even more important role in a correct explanation of the data.

V. CONCLUSION

In this paper we have presented a quantitative analysis of the quantum fluctuations in the vortex system of high-temperature superconductors. Starting from the vortex equation of motion, we have derived the effective Euclidean action for the vortex system, which replaces the elastic free energy as the basic functional when going over from the classical to the quantum statistical mechanics. We then have used this formalism in order to calculate the specific heat and the reversible magnetic "susceptibility" of the vortex lattice at low temperatures. Second, we have determined the effect of quantum fluctuations on the shape of the melting transition of the vortex lattice.

The calculation of the vortex specific heat has been based on the determination of the translational fluctuation energy. For a dissipative dynamics the vortex contribution to the specific heat is linear in T at low temperatures and shows a field dependence $\propto \sqrt{B}/\ln B$ for low and $\propto \ln B$ for high magnetic fields. For the Hall dynamics relevant in superclean material the specific heat is determined by the Tkachenko waves; in the single-vortex regime the result is linear in field and shows a $T^{1/2}$ temperature dependence. These results have to be compared with the specific-heat contribution from the normal core regions[26] which also scales linearly in T but shows a linear dependence on field (for the superclean situation the minigap $\hbar\omega_0$ suppresses this linear term at low temperatures $T<\hbar\omega_0$). A third contribution to the specific heat and related to the presence of vortices in the system is due to fluctuations of the order parameter (self-fluctuations[64]) and we have not considered this term here. In addition, these vortex contributions compete with the quasiparticle and the phonon specific heat, where the quasiparticle contribution also can exhibit a power-law dependence in T, e.g., $C_{vc} \propto T$ for the quasiparticles in the vortex cores and $C_{vqp} \propto T^2 (T^3)$ if the gap itself exhibits line (point) nodes. In summary, then, it appears to be rather difficult but not impossible to single out the vortex contribution to the specific heat.

The low-temperature magnetic "susceptibility" $\chi = \partial M/\partial \ln H$ is predicted by mean-field London theory to be a constant in the intermediate field regime $0.01 H_{c2} \lesssim H \lesssim 0.3 H_{c2}$. Taking the suppression of the order parameter (vortex cores) into account[42] results in a reduction of χ with increasing field. However, this effect alone cannot explain the experimentally observed reduction in χ with increasing field,[17] which amounts to $\sim 50\%$ at a field of 7 T (BiSCCO, $T=35$ K). Taking quantum fluctuations into account we can explain this decrease in χ using a set of parameters consistent with theoretical and experimental expectations (including also those obtained from quantum creep phenomena).

The description of the melting transition has been based on the Lindemann criterion, saying that the lattice melts when the mean squared displacement amplitude becomes of the order of the lattice constant. We have argued that away from the transition temperature T_c the quantum fluctuations do contribute to the melting process and hence should be included in the calculation of the mean squared displacement amplitude of the vortex lattice. The comparison between theory and experiment can be done at different levels of accuracy and we have tested the various thermal theories against our result including also quantum effects: The most simple thermal expression $B_m \propto (T_c/T-1)^2$ turns out to give only a very poor agreement with the experimental data. A considerable improvement has been obtained by using the more accurate thermal result by Houghton, Pelcovits, and Sudbø[5] which takes into account the suppression $\propto (1-B/H_{c2})$ of the order parameter on approaching the upper critical field line H_{c2}. A further improvement between the thermal theory and experiment has been obtained by additionally accounting for the saturation of the Ginzburg-Landau parameters ξ and λ at low temperatures as described by the temperature dependence $(1-T^2/T_c^2)/2$. This modified thermal theory then has provided good agreement with the experimental melting

line as measured in a BiSCCO single crystal over a very large temperature range $T_c/2 < T < T_c$. In order to obtain good agreement with the experimental melting line measured in various YBCO single crystals we had to include effects of quantum fluctuations, which is consistent with theoretical expectations. Whereas the thermal displacement amplitude scales with (the square root of) the Ginzburg number $\langle u^2 \rangle_{th} \propto \sqrt{G}$, the quantum contribution $\langle u^2 \rangle_q \propto Q$ is proportional to the quantum parameter Q. The Ginzburg number G differs by roughly three orders of magnitude between the Y- and Bi-based materials, whereas the quantum parameter Q remains essentially unchanged. Hence in BiSCCO the thermal fluctuations are clearly dominant and the thermal result of Houghton, Pelcovits, and Sudbø is well applicable within the 3D regime $B < B_{2D}$. On the other hand, in YBCO, quantum fluctuations do contribute to the mean squared displacement field and should be taken into account for an accurate description of the melting line. Note that the parameters used in the explanation of a variety of quantum phenomena in the vortex system of high-temperature superconductors (quantum creep, reversible magnetization, melting) are consistent overall.

In the above analysis we have neglected the effect of quenched disorder and have treated the melting transition in a pure system. The presence of weak quenched disorder is expected to assist the quantum fluctuations in the suppression of the melting line towards smaller temperatures and fields. The quantitative treatment on an equal footing of both these effects remains an interesting task.

ACKNOWLEDGMENTS

We wish to thank D. Farrell, M. Feigel'man, V. Geshkenbein, R. Griessen, H.-R. Ott, T. M. Rice, and H. Safar for stimulating and helpful discussions. We are particularly grateful to H.-R. Ott and to H. Safar for providing us with their data prior to publication. One of us (B.I.) thanks the Swiss National Foundation for financial support.

*Present address: Universidad Autonoma de San Luis Potosi, Instituto de Fisica, Alvaro Obregon 64, 78000 San Luis Potosi, S. L. P. Mexico.

[1]D. S. Fisher, M. P. A. Fisher, and D. A. Huse, Phys. Rev. B **43**, 130 (1991).

[2]G. Blatter, M. V. Feigel'man, V. B. Geshkenbein, A. I. Larkin, and V. M. Vinokur, Rev. Mod. Phys. (to be published).

[3]D. R. Nelson, Phys. Rev. Lett. **60**, 1973 (1988).

[4]E. H. Brandt, Phys. Rev. Lett. **63**, 1106 (1989).

[5]A. Houghton, R. A. Pelcovits, and A. Sudbø, Phys. Rev. B **40**, 6763 (1989).

[6]P. L. Gammel, L. F. Schneemeyer, J. V. Waszczak, and D. J. Bishop, Phys. Rev. Lett. **61**, 1666 (1988).

[7]H. Safar, P. L. Gammel, D. A. Huse, D. J. Bishop, J. P. Rice, and D. M. Ginsberg, Phys. Rev. Lett. **69**, 824 (1992).

[8]Y. Yeshurun and A. P. Malozemoff, Phys. Rev. Lett. **60**, 2202 (1988).

[9]L. Fruchter, A. P. Malozemoff, I. A. Campbell, J. Sanchez, M. Konczykowski, R. Griessen, and F. Holtzberg, Phys. Rev. B **43**, 8709 (1991).

[10]A.-C. Mota, G. Juri, P. Visani, A. Pollini, T. Teruzzi, K. Aupke, and B. Hilti, Physica C **185-189**, 343 (1991).

[11]R. Griessen, J. G. Lensink, and H. G. Schnack, Physica C **185-189**, 337 (1991).

[12]G. Blatter, V. B. Geshkenbein, and V. M. Vinokur, Phys. Rev. Lett. **66**, 3297 (1991).

[13]B. I. Ivlev, Yu. N. Ovchinnikov, and R. S. Thompson, Phys. Rev. B **44**, 7023 (1991).

[14]M. V. Feigel'man, V. B. Geshkenbein, A. I. Larkin, and S. Levit, Pis'ma Zh. Eksp. Teor. Fiz. **57**, 699 (1993) [JETP Lett. **57**, 711 (1993)].

[15]G. Blatter and B. Ivlev, Phys. Rev. Lett. **70**, 2621 (1993).

[16]L. N. Bulaevskii and M. P. Maley, Phys. Rev. Lett. **71**, 3541 (1993).

[17]L. N. Bulaevskii, J. H. Cho, M. P. Maley, P. Kes, Q. Li, M. Suenaga, and M. Ledvij, Phys. Rev. B **50**, 3507 (1994).

[18]H. Safar, P. L. Gammel, D. A. Huse, D. J. Bishop, W. C. Lee, and D. M. Ginsberg, Phys. Rev. Lett. **70**, 3800 (1993).

[19]H. Safar (private communication).

[20]A. Schilling, H. R. Ott, and Th. Wolf, Phys. Rev. B **46**, 14 253 (1992).

[21]A. Schilling, R. Jin, J. D. Guo, H. R. Ott, I. Tanaka, and H. Kojima, in *Proceedings of the XXth International Conference on Low Temperature Physics, Eugene, Oregon, 1993* [Physica B **194-196**, 1555 (1994)].

[22]E. H. Brandt and U. Essmann, Phys. Status Solidi B **144**, 13 (1987).

[23]N. B. Kopnin and V. E. Kravtsov, Zh. Eksp. Teor. Fiz. **71**, 1644 (1976) [Sov. Phys. JETP **44**, 861 (1976)].

[24]N. B. Kopnin and V. E. Kravtsov, Pis'ma Zh. Eksp. Teor. Fiz. **23**, 631 (1976) [JETP Lett. **23**, 578 (1976)].

[25]N. B. Kopnin and M. M. Salomaa, Phys. Rev. B **44**, 9667 (1991).

[26]C. Caroli, P. B. De Gennes, and J. Matricon, Phys. Lett. **9**, 307 (1964).

[27]V. M. Vinokur, V. B. Geshkenbein, M. V. Feigel'man, and G. Blatter, Phys. Rev. Lett. **71**, 1242 (1993).

[28]J. Bardeen and R. Sherman, Phys. Rev. B **12**, 2634 (1975).

[29]J. Bardeen and M. J. Stephen, Phys. Rev. **140**, A1197 (1965).

[30]L. P. Gor'kov and N. B. Kopnin, Zh. Eskp. Teor. Fiz. **65**, 396 (1973) [Sov. Phys. JETP **38**, 195 (1974)].

[31]A. I. Larkin and Yu. N. Ovchinnikov, in *Nonequilibrium Superconductivity,* edited by D. N. Langenberg and A. I. Larkin (Elsevier, Amsterdam, 1986), p. 493.

[32]Z. Schlesinger, R. T. Collins, R. Holtzberg, C. Field, S. H. Blanton, U. Welp, G. W. Crabtree, Y. Fang, and J. Z. Liu, Phys. Rev. Lett. **65**, 801 (1990).

[33]A. I. Larkin and Yu. N. Ovchinnikov, Pis'ma Zh. Eksp. Teor. Fiz. **37**, 322 (1983) [JETP Lett. **37**, 382 (1983)].

[34]R. P. Feynman and A. R. Hibbs, *Quantum Mechanics and Path Integrals* (McGraw-Hill, New York, 1965).

[35]V. K. Tkachenko, Zh. Eksp. Teor. Fiz. **50**, 1573 (1966) [Sov. Phys. JETP **23**, 1049 (1966)].

[36]V. K. Tkachenko, Zh. Eksp. Teor. Fiz. **56**, 1763 (1969) [Sov.

Phys. JETP **29**, 945 (1969)].
[37]E. B. Sonin, Rev. Mod. Phys. **59**, 87 (1987).
[38]N. P. Ong (private communication).
[39]H. Suhl, Phys. Rev. Lett. **14**, 226 (1965).
[40]M. W. Coffey, Phys. Rev. B **49**, 9774 (1994).
[41]Ji-Min Duan and E. Šimánek, Phys. Lett. A **190**, 118 (1994).
[42]Z. Hao and J. Clem, Phys. Rev. Lett. **67**, 2371 (1991); Phys. Rev. B **43**, 2844 (1991).
[43]K. Aupke, T. Teruzzi, P. Visani, A. Amann, A.-C. Mota, and V. N. Zavaritsky, Physica C **209**, 255 (1993).
[44]D. Prost, L. Fruchter, I. A. Campbell, N. Motohira, and M. Konczykowski, Phys. Rev. B **47**, 3957 (1993).
[45]M. N. Kunchur, D. K. Christen, and J. M. Phillips, Phys. Rev. Lett. **70**, 998 (1993).
[46]H.-R. Ma and S. T. Chui, Phys. Rev. Lett. **67**, 505 (1991).
[47]Y.-H. Li and S. Teitel, Phys. Rev. Lett. **66**, 3301 (1991).
[48]S. Ryu, S. Doniach, G. Deutscher, and A. Kapitulnik, Phys. Rev. Lett. **68**, 710 (1992).
[49]S. Sengupta, C. Dasgupta, H. R. Krishnamurthy, G. I. Menon, and T. V. Ramakrishnan, Phys. Rev. Lett. **67**, 3444 (1991).
[50]S. Hikami, A. Fujita, and A. I. Larkin, Phys. Rev. B **44**, 10 400 (1991).
[51]F. Lindemann, Phys. Z. (Leipzig) **11**, 69 (1910).
[52]L. P. Gor'kov and G. M. Eliashberg, Zh. Eksp. Teor. Fiz. **54**, 612 (1968) [Sov. Phys. JETP **27**, 328 (1968)].
[53]B. I. Ivlev and N. B. Kopnin, Adv. Phys. **33**, 47 (1984).
[54]M. Tinkham and J. Clarke, Phys. Rev. Lett. **28**, 1366 (1972).
[55]J. Clarke, Phys. Rev. Lett. **28**, 1363 (1972).
[56]U. Welp, W. K. Kwok, G. W. Crabtree, K. G. Vandervoort, and J. Z. Liu, Phys. Rev. Lett. **62**, 1908 (1989).
[57]U. Welp, S. Fleshler, W. K. Kwok, R. A. Klemm, V. M. Vinokur, J. Downey, B. Veal, and G. W. Crabtree, Phys. Rev. Lett. **67**, 3180 (1991).
[58]D. Ceperley, Phys. Rev. B **18**, 3126 (1978).
[59]K. A. Müller, M. Takashige, and J. G. Bednorz, Phys. Rev. Lett. **58**, 1143 (1987).
[60]D. E. Farrell, J. P. Rice, and D. M. Ginsberg, Phys. Rev. Lett. **67**, 1165 (1991).
[61]L. Krusin-Elbaum, L. Civale, F. Holtzberg, A. P. Malozemoff, and C. Feild, Phys. Rev. Lett. **67**, 3156 (1991).
[62]G. Blatter, B. Ivlev, Yu. Kagan, M. Theunissen, Y. Volokitin, and P. Kes, Phys. Rev. B (to be published).
[63]D. A. Brawner, A. Schilling, H. R. Ott, R. J. Haug, K. Ploog, and K. von Klitzing, Phys. Rev. Lett. **71**, 785 (1993).
[64]G. Blatter, B. Ivlev, and H. Nordborg, Phys. Rev. B **48**, 10 448 (1993).